Bias effect in photocurrent response of Si nanocrystals

R. Zhang,[1,a)] X. Y. Chen,[2] and W. Z. Shen[2,b)]
[1]*Division of Basic Courses, Shanghai Maritime University, Shanghai 200135, People's Republic of China*
[2]*Department of Physics, Laboratory of Condensed Matter Spectroscopy and Opto-Electronic Physics, Shanghai Jiao Tong University, 1954 Hua Shan Road, Shanghai 200030, People's Republic of China*

(Received 8 October 2008; accepted 18 December 2008; published online 13 February 2009)

We report on the photocurrent response of hydrogenated nanocrystalline silicon (nc-Si:H) thin films under external bias voltages. The band gap transition and internal photoemission photocurrent of the nc-Si:H thin films can be enhanced and controlled by adjusting the depletion and inversion layers in the metal-semiconductor junction through the external bias voltage. The photocurrent response from the internal photoemission is found to be able to extend the photodetection wavelength of the Si material to the optical telecommunication range of 1.3–1.6 μm. © *2009 American Institute of Physics*. [DOI: 10.1063/1.3075760]

I. INTRODUCTION

Photoluminescence properties of hydrogenated nanocrystalline silicon (nc-Si:H) thin films have attracted considerable interest because silicon nanometer crystals can emit strong luminescence at room temperature with adjustable band gap energy from bulk Si band gap (1.12 eV) to the visible region by controlling the grain size.[1,2] Especially, the luminescence energy can also be tuned to the optical telecommunication wavelength range of 1.3–1.6 μm by impurity doping.[3] Nevertheless, it should be noted that the carrier transport is prohibited between these isolated Si nanocrystals. In order to observe the photocarrier transition and collection in the Si nanocrystal system, the distance among the Si nanocrystals must be close enough to permit electron transmission.

Recently, we have established a way to obtain a nc-Si:H thin film consisting of high density of Si grains (10 nm or less in size) separated by the very narrow amorphous silicon (*a*-Si) boundaries produced by plasma-enhanced chemical vapor deposition (PECVD) under optimal growth conditions.[4–6] In the nc-Si:H thin film with high density of Si nanocrystals, the conductivity can be improved to a range of $\sim 10^{-2}$–10^{2} Ω^{-1} cm^{-1}, much higher than that of *a*-Si or *a*-Si:H materials in the range of $\sim 10^{-11}$–10^{-4} Ω^{-1} cm^{-1}.[7,8] The improvement of electronic transport in the nc-Si:H thin film is caused by the high density of nanocrystals, which yields the electronic wave-function overlapping and results in an energy subband with continuous states. This argument has recently been demonstrated by the high photocurrent response due to the transitions of the subband.[9,10] The nc-Si:H thin film with high density of both Si crystals and *a*-Si boundaries in nanometer level is found to be good not only for electronic transport, but also for photocurrent response. The high photocurrent response leads to a wide range of potential optoelectronic applications with improved performance, such as the infrared detection and imaging application.[11,12]

In this paper, we report on the bias effect in the photocurrent response of the high-quality nc-Si:H thin films on glass substrates by PECVD. We will show that the band gap transition within the nanometer Si grains dominates the observed photocurrent response, and the photocurrent is controlled by the external bias voltages. Through the reverse bias voltage control of the depletion layer, we demonstrate not only the improvement of the photocurrent response, but also the extension of the response into the optical telecommunication range of 1.3–1.6 μm through the internal photoemission under reverse bias.

II. SAMPLE GROWTH AND STRUCTURAL CHARACTERIZATION

The studied nc-Si:H thin film samples were grown by the PECVD system reported elsewhere.[9,10] The samples were deposited at 250 °C under the chamber pressure of 1.0 Torr. The percentage content of silane (SiH_4/SiH_4+H_2) is about 1.0% and the deposition rate is as low as about 0.3 Å/s under the present hydrogen dilution. The surface of the nc-Si:H thin films has been characterized by atomic force microscopy (AFM), which was performed on BioScope atomic force microscope of Veeco Instruments Inc. The depletion layer of the studied sample under external bias has been investigated through the capacitance-voltage measurement by an electrical system including Agilent 4284A *LCR* meter, 15065 external bias testing fixture, and Keithley 2400 source meter. The photocurrent spectra have been acquired using a Nicolet Nexus 870 Fourier transform infrared spectrometer.

Figure 1 shows a typical AFM image of the nc-Si:H thin film surface, which clearly identifies the constitution of grains in nanometer level from the viewpoint of the surface of the film. Our previous x-ray diffraction experimental results[9] also show two clear diffraction peaks of (111) and (220), together with a dim (331) peak of Si, and the average grain sizes of Si nanocrystals ($D_{(220)}$) of 2.9 nm can be obtained from the diffraction peaks by using the Scherrer formula.[13] These results shows the good quality and stability

a)Author to whom correspondence should be addressed. Electronic mail: rongzhang@dbc.shmtu.edu.cn.
b)Electronic mail: wzshen@sjtu.edu.cn.

 © 2009 American Institute of Physics

Author complimentary copy. Redistribution subject to AIP license or copyright, see http://jap.aip.org/jap/copyright.jsp

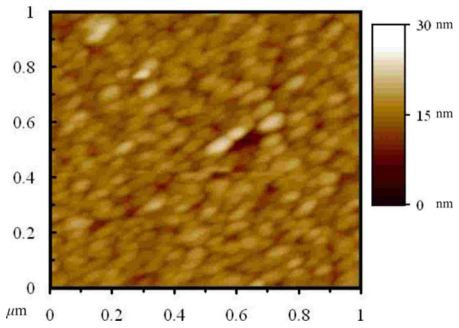

FIG. 1. (Color online) AFM image of the surface of the studied nc-Si:H thin film.

of the studied nc-Si:H film whose thickness was about 1.0 μm and with hydrogen content of ~5.0% revealed by elastic recoil detection analysis.[5]

III. RESULTS AND DISCUSSIONS

Figure 2 presents the room-temperature photocurrent spectra of the nc-Si:H thin film sample measured under a series of applied (a) forward and [(b) and (c)] reverse bias voltages. Here, the experimental photocurrent signal turns to be a main photocurrent peak for the photon energy over 1.05 eV, and the amplitude of the main peak increases monotonously with the external bias voltage. It should be noted that the photocurrent at photon energy above 1.05 eV has been demonstrated to be caused by the high crystalline fraction in the nc-Si:H thin films, as discussed in Ref. 9. Moreover, the electron-hole pair generation from the electronic transitions with photon energy above 1.05 eV has also been proved by the experimental result of a negative photocapacitance reported in Ref. 14. Therefore, we can assign the photon energy of 1.05 eV to be the band gap energy and the photocurrent above the band gap energy to be the contribution from the electron-hole pairs generated from the electronic transitions within the Si nanometer grains, because the high density of nanometer Si crystals is a prerequisite condition to form such a main photocurrent peak at the photon energy threshold of 1.05 eV in the nc-Si:H thin films.[9,10] Especially, such a threshold photon energy of 1.05 eV in photocurrent spectrum of the nc-Si:H thin film is very close to the band gap of crystalline Si and much lower than that of *a*-Si material (above 1.6 eV), which allows us to tune the band gap of nc-Si thin films by adjusting the physical microstructure of grains and voids.[10,12]

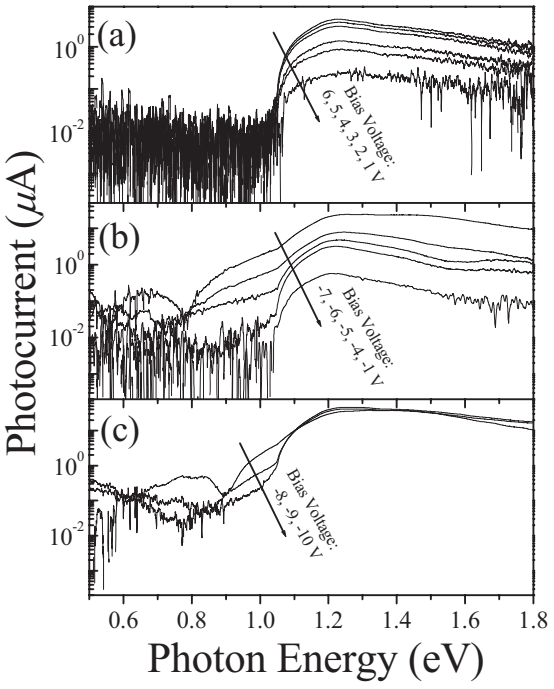

FIG. 2. Room-temperature photocurrent spectra (in logarithmic scale) of the nc-Si:H thin film sample under (a) positive bias voltages of 1, 2, 3, 4, 5, and 6 V; (b) reverse bias voltages of −1, −4, −5, −6, and −7 V; and (c) reverse bias voltages of −8, −9, and −10 V.

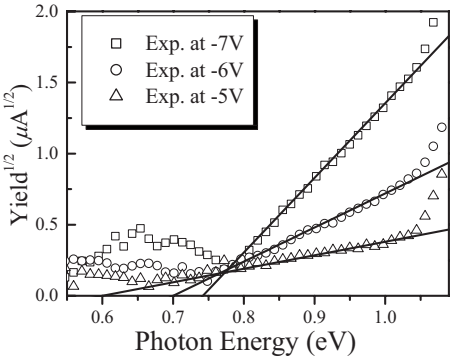

FIG. 3. Experimental photocurrents of the nc-Si:H thin film under reverse bias voltages of −5, −6, and −7 V. Solid lines are the internal photoemission calculation results.

The photocurrent spectra in Fig. 2(b) display distinguishable protruding plateaus for the photon energy below the band gap energy under the reverse bias beyond −4 V. The photocurrent plateau below the band gap energy has not been observed under the forward bias voltages in Fig. 2(a), indicating its relation to the depletion region at the interface between the metal contacts and the nc-Si:H thin film under the reverse bias voltage. The origin of the protruding plateaus on the photocurrent spectra will be explained well below by the special relation between photocurrent and reverse bias voltages.

Figure 3 shows the squared collection efficiency *Y*, defined as photocurrent per photon incident on the metal, as a function of photon energy under different reverse biases. It is fitted very well by the standard form for internal photoemission:[15]

$$Y(E) = A(E - E_b)^2 \propto I_{\mathrm{ph}}, \tag{1}$$

where E is the photon energy and A is a constant determined by the number of photons absorbed and the escape probability of an excited electron in the metal. The values of the Schottky barrier height E_b determined by the straight lines in Fig. 3 are 0.75, 0.70, and 0.60 eV for the biases of −7, −6, and −5 V, respectively. These obtained Schottky barrier heights E_b are also in the same magnitude of those reported in the *a*-Si:H thin film.[16] Therefore, the parabolic relation of the low-energy photocurrent is attributed to be the internal photoemission from the metal contact indium into the semiconducting nc-Si:H thin film, as previously reported in Refs.

Author complimentary copy. Redistribution subject to AIP license or copyright, see http://jap.aip.org/jap/copyright.jsp

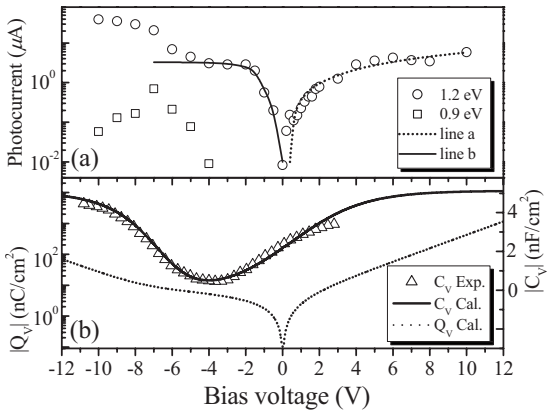

FIG. 4. (a) Experimental photocurrents at photon energies of 1.2 eV (circles) and 0.9 eV (squares) of the nc-Si:H thin film plotted as a function of bias voltage. Curves a and b are the theoretical calculation results. (b) Experimental capacitance-voltage characteristics (triangles), together with the calculated capacitances (solid curve) and charge densities (dotted curve).

16 and 17. The interfacial depletion layer within the metal-semiconductor (M-S) junction depends strongly on the bias voltage, which results in the following photocurrent characteristics of band transition and internal photoemission with the external bias voltage.

Figure 4(a) illustrates the photocurrent amplitude at fixed photon energies of 0.9 eV (empty squares) and 1.2 eV (empty circles) as a function of the external bias voltage V. The photocurrent intensity at the photon energy of 1.2 eV increases monotonously with the positive bias voltage. The higher the forward bias voltage applied between the two contacts is, the more the photocarriers generated by the band gap transmission will transit over the semiconducting film because both the electrons and holes can be injected into the material from the contacts to maintain charge neutrality of the film. Therefore, the photocurrent (I_{ph}) at the photon energy of 1.2 eV can be well explained by the linear formula $I_{ph} \propto V$, as demonstrated by the good agreement between empty circles and dotted curve a in Fig. 4(a). Unlike the photocurrent from the band transition at 1.2 eV, the photocurrent from the internal photoemission at 0.9 eV disappears in the background noise signals under forward bias voltages [see Fig. 2(a)], but only appears under reverse bias voltages over −4 V.

Under reverse bias voltages, the photocurrent from the band transition at 1.2 eV shows two distinguishable jump-increases with the bias voltage. It should be noted that the first photocurrent jump-increase at the beginning of the reverse bias voltage in Fig. 4(a) is accompanied by the same increase in interfacial charge density (Q_V) in Fig. 4(b). With the increase in the reverse bias voltage, the positive charge within the depletion layer of the M-S interface increases with the depletion layer width. It is the increase in the depletion width W that causes the first jump-increase in the photocurrent below the bias voltage of −2 V. Therefore, the first photocurrent jump-increase from the band transition at 1.2 eV is well fitted by the formula

$$I_{ph} \propto 1 - \exp(-\alpha W) = 1 - \exp(-\alpha W_0 \sqrt{V}), \quad (2)$$

where α is absorption coefficient and W_0 is width of the depletion layer at a voltage V across it,[18,19] as revealed by the solid curve b in Fig. 4(a) Another jump-increase in the photocurrent from band transition under high reverse bias voltages is related to the inversion layer, as discussed below.

Figure 4(b) presents the experimental bias dependent capacitance (triangles) of the studied sample measured with a frequency of 100 Hz, together with the calculated results of M-S interface charge (dotted curve) and its differential capacitance (solid curve), for the typical M-S junction structure as a function of bias voltage.[20] The good agreement between the scatters and solid curve demonstrates that the M-S interface capacitance of the nc-Si:H thin film also fits well with the traditional semiconductor depletion theory. Both the M-S interfacial charge and its differential capacitance exhibit distinguishable asymmetry in the results versus bias voltage due to the asymmetry of the M-S junction and depletion layer structure. With the reverse bias voltage increasing, the width of the depletion layer at the interface between metal contacts and nc-Si:H thin film increases, resulting in a decrease in the capacitance. With a further increase in the reverse bias voltage, an inversion layer develops after the depletion layer is saturated, as evidenced by the increase in the interfacial charge for reverse bias voltages beyond −4 V in Fig. 4(b). It is clear that the minimum point of the M-S interfacial capacitance indicates the saturation of the depletion layer and the formation of inversion layer at the M-S interface.

Under reverse bias voltage, the internal photoemission appears only after the inversion layer is formed, as revealed in Fig. 4, where the photocurrent from internal photoemission is observed to increase with the positive charge in the inversion layer. However, it decreases with bias voltage because the electrons from the metal contacts to the nc-Si:H thin film are transferred from photoemission to direct tunneling with further increase in the reverse bias voltage. Therefore, the internal photoemission photocurrent increases with the Schottky barrier under low reverse bias, but decreases under high reverse bias when the Schottky barrier becomes narrow enough to result in the tunneling transport dominating the photocarrier collection. Therefore, the internal photoemission photocurrent shows a maximum with the reverse bias, as shown by the squares in Fig. 4(a). The photon energy range (0.7–1.0 eV) of the internal photoemission photocurrent observed in Fig. 2(b) matches well with the optical telecommunication range of 1.3–1.6 μm, indicating the potential application of the nc-Si:H thin film in the optical telecommunication field. It is the tunneling transport that causes the disappearance of the internal photoemission, but enhancing significantly the photocurrent from the band gap transition, as shown by the circles in Fig. 4(a).

Figure 5 presents the photocurrent spectra under high reverse bias voltages beyond 6 V, where some weak fringes can be observed. Usually, the interference fringe in the photocurrent spectra is limited by the thickness and photon absorption of the thin film. In the studied nc-Si:H thin film with 1 μm thickness, the high photocarrier collection efficiency due to inversion layer and the tunneling transport result in the weak fringes observable in the photocurrent spectra under high reverse bias, which also agrees with the theoretical result of Eq. (3) of Ref. 9. This clearly indicates that the high

Author complimentary copy. Redistribution subject to AIP license or copyright, see http://jap.aip.org/jap/copyright.jsp

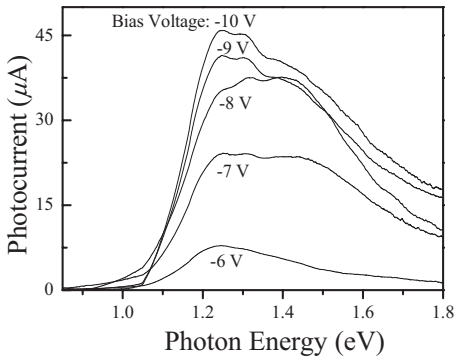

FIG. 5. Experimental photocurrent spectra of the nc-Si:H thin film under reverse bias voltages ranging from −6 to −10 V.

reverse bias can significantly enhance the photocurrent response of the nc-Si:H thin film, and even allows it to detect the interference fringes in the thin film.

IV. CONCLUSIONS

We have demonstrated the bias effect on the photocurrent from the band gap transition and the internal photoemission in the nc-Si:H thin films. The reverse bias voltage is found to be able to hugely help the photocarrier collection due to the depletion layer and inversion layer formation at the M-S interface. Especially, the photocurrent from the internal photoemission is observed within the photon energy ranging from 0.8 to 1.0 eV due to the suitable Schottky barrier height and width under reverse bias voltage ranging from 5 to 7 V. The high photocurrent response under reverse bias voltage allows us to apply the nc-Si:H thin film on the photodetection devices, even in the field of the optical telecommunication range of 1.3–1.6 μm through the internal photoemission.

ACKNOWLEDGMENTS

This work was supported by the NSF of China under Contract No. 10674094, the Shanghai Municipal Commission of Science and Technology under Project No. 08XD14022, the Innovation Program of Shanghai Municipal Education Commission under Contract No. 09YZ238, and the Expenditure Budget Program of Shanghai Municipal Education Commission under Contract No. 2008074, as well by Shanghai Maritime University under the excellent Young Teachers' Plan No. 025063.

[1] M. Fujii, A. Mimura, S. Hayashi, Y. Yamamoto, and K. Murakami, Phys. Rev. Lett. **89**, 206805 (2002).
[2] S. Takeoka, M. Fujii, and S. Hayashi, Phys. Rev. B **62**, 16820 (2000).
[3] M. Fujii, K. Toshikiyo, Y. Takase, Y. Yamaguchi, and S. Hayashi, J. Appl. Phys. **94**, 1990 (2003).
[4] Y. L. He, G. Y. Hu, M. B. Yu, M. Liu, J. L. Wang, and G. Y. Xu, Phys. Rev. B **59**, 15352 (1999).
[5] X. Y. Chen, W. Z. Shen, and Y. L. He, J. Appl. Phys. **97**, 024305 (2005); M. H. Gullanar, H. Chen, W. S. Wei, R. Q. Cui, and W. Z. Shen, *ibid.* **95**, 3961 (2004).
[6] S. C. Saha and S. Ray, J. Appl. Phys. **78**, 5713 (1995).
[7] R. Brüggemann, J. P. Kleider, C. Longeaud, D. Mencaraglia, J. Guillet, J. E. Bourée, and C. Niikura, J. Non-Cryst. Solids **266–269**, 258 (2000).
[8] M. H. Brodsky, R. S. Title, K. Weiser, and G. D. Pettit, Phys. Rev. B **1**, 2632 (1970).
[9] R. Zhang, X. Y. Chen, K. Zhang, and W. Z. Shen, J. Appl. Phys. **100**, 104310 (2006).
[10] R. Zhang, X. Y. Chen, and W. Z. Shen, Proc. SPIE **6984**, 69842U (2008).
[11] M. Tucci and R. DeRosa, Solid-State Electron. **44**, 1315 (2000).
[12] H. Mimura and Y. Hatanaka, J. Appl. Phys. **61**, 2575 (1987).
[13] M. R. Fitzsimmons, J. A. Eastman, M. Müller-Stach, and G. Wallner, Phys. Rev. B **44**, 2452 (1991).
[14] D. Kwon, C. C. Chen, J. D. Cohen, H. C. Jin, E. Hollar, I. Robertson, and J. R. Abelson, Phys. Rev. B **60**, 4442 (1999).
[15] S. M. Sze, *Physics of Semiconductor Devices* (Wiley, New York, 1969), p. 404.
[16] C. R. Wronski, B. Abeles, G. D. Cody, and T. Tiedje, Appl. Phys. Lett. **37**, 96 (1980).
[17] W. B. Jackson, R. J. Nemanich, and N. M. Am, Phys. Rev. B **27**, 4861 (1983).
[18] W. W. Gartner, Phys. Rev. **116**, 84 (1959).
[19] R. S. Crandall, R. Williams, and B. E. Tompkins, J. Appl. Phys. **50**, 5506 (1979).
[20] R. H. Kingston and S. F. Neustadter, J. Appl. Phys. **26**, 718 (1955).

Author complimentary copy. Redistribution subject to AIP license or copyright, see http://jap.aip.org/jap/copyright.jsp